Front. Optoelectron. 2019, 12(4): 344–351
https://doi.org/10.1007/s12200-019-0904-7

RESEARCH ARTICLE

Screen printing process control for coating high throughput titanium dioxide films toward printable mesoscopic perovskite solar cells

Zhining WAN*, Mi XU*, Zhengyang FU, Da LI, Anyi MEI, Yue HU, Yaoguang RONG (✉), Hongwei HAN

Michael Grätzel Center for Mesoscopic Solar Cells, Wuhan National Laboratory for Optoelectronics, China-EU Institute for Clean and Renewable Energy, Huazhong University of Science and Technology, Wuhan 430074, China

Abstract Screen printing technique has been widely applied for the manufacturing of both traditional silicon solar cells and emerging photovoltaics such as dye-sensitized solar cells (DSSCs) and perovskite solar cells (PSCs). Particularly, we have developed a printable mesoscopic PSC based on a triple layer scaffold of TiO_2/ZrO_2/carbon. The deposition of the scaffold is entirely based on screen printing process, which provides a promising prospect for low-cost photovoltaics. However, the optimal thickness of the TiO_2 layer for fabricating efficient printable PSCs is much smaller than the typical thickness of screen printed films. Here, we tune the concentration of the pastes and the printing parameters for coating TiO_2 films, and successfully print TiO_2 films with the thickness of 500 – 550 nm. The correlation between the thickness of the films and printing parameters such as the solid content and viscosity of the pastes, the printing speed and pressure, and the temperature has been investigated. Besides, the edge effect that the edge of the TiO_2 films possesses a much larger thickness and printing positional accuracy have been studied. This work will significantly benefit the further development of printable mesoscopic PSCs.

Keywords screen printing, perovskite solar cells (PSCs), thickness, parameter control

1 Introduction

Screen printing technique has been widely used in different industries, including clothing, product labels, signs, textile fabric, printed electronics and so on [1,2]. One of the parameters that can vary and can be fine controlled in screen printing is the thickness of the print films or patterns [3,4]. This makes it useful for some of the techniques of printing electronics etc. Particularly, the manufacturing of traditional silicon solar cells and emerging photovoltaics of mesoscopic solar cells involves the process based on screen printing [5–7].

The 1st generation mesoscopic solar cells of dye-sensitized solar cells (DSSCs) [8,9] are based on a sandwich structure of fluorine-doped tin oxide (FTO)/mesoporous TiO_2/electrolyte/Platinum electrode/FTO. Since the TiO_2 layer (10 – 12 μm) can be deposited with screen printing process [7,9], the manufacturing of DSSCs is easy to scale up [10–12]. Various large-area DSSC modules and panels based on screen printing fabrication process have been reported, providing promising prospect for practical applications [13–16]. The 2nd generation mesoscopic solar cells of perovskite solar cells (PSCs) employ organic-inorganic hybrid trihalide perovskites (typically $CH_3NH_3PbI_3$) as the light absorbers [17], and usually possess a monolithic structure of FTO/electron transport layer (ETL)/perovskite/hole transport layer (HTL)/Au [18–20]. Currently, PSCs have achieved a certified power conversion efficiency (PCE) of 23.7% in laboratory-scale [21,22]. To further explore the potential commercialization, intensive research has been focused on the stability and upscaling of PSCs [23–27]. Depending on the sequence of depositing the ETL and HTL, the device structure can be divided into formal (conventional) versus inverted architectures [28,29]. Particularly, we have reported a triple mesoscopic structure based on the scaffold of TiO_2/ZrO_2/carbon for PSCs [30]. Since the deposition of the scaffold is entirely based on screen printing process, this type of PSCs is simply named as printable PSCs. Currently, this type of PSCs has demonstrated quite

Received January 29, 2019; accepted February 17, 2019

E-mail: ygrong@hust.edu.cn

*These authors contributed equally to this work.

promising potential for the commercialization and attracted much research attention [31–34].

For fabricating efficient printable PSCs, the optimal thickness of the TiO_2 layer, ZrO_2 layer and carbon layer of the scaffold are ~500 nm, ~3 μm and 10 μm, respectively [35]. As usual, it is implementable for screen printing technique to deposit micrometer-thick films, such as the silver grids for silicon solar cell cells and TiO_2 electrodes for DSSCs. However, to deposit nanometer-thick films by screen printing technique, it is challenging to precisely control the thickness and uniformity.

Here, we tune the concentration of the printing pastes and printing parameters for coating TiO_2 films, and successfully print TiO_2 films with the thickness of 500 – 550 nm and minimize the thickness errors. The correlation between the thickness of the films and printing parameters such as the solid content and viscosity of the pastes, the printing speed and pressure, and the temperature has been investigated. Besides, the edge effect that the edge of the TiO_2 films possesses a much larger thickness and printing positional accuracy have been studied.

2 Experimental section

2.1 Materials

Unless stated otherwise, all materials were purchased from Sigma-Aldrich. The TiO_2 was purchased from GreatCell Solar or WonderSolar. The ZrO_2 and carbon pastes were provided by WonderSolar.

2.2 Printing of the films

FTO glass substrates were etched with a 1064 nm laser, and then ultrasonically cleaned with detergent, deionized water and ethanol for 10 min, respectively. The screen printer (SMT-DEK, icon 6) has an automatic sample loading system and a CCD automatic positioning system. The parameters of the screen mesh are as: 150T mesh/inch; tension 25 N/cm; polyester thread with a diameter of 45 μm. The printing parameters are as: printing speed 50–250 mm/s; printing gap: 2 – 4 mm; printing pressure: 4 – 10 kg. After printing, the films were sintered at 500°C for 30 min.

3 Results and discussion

The printable mesoscopic PSCs based on TiO_2/ZrO_2/carbon triple-layer were fabricated using screen printing techniques, as shown in Fig. 1. The TiO_2 layer, ZrO_2 layer and carbon layer were screen printed on the FTO substrate layer by layer. The perovskite absorber was infiltrated in the mesoporous scaffold by a simple solution casting method, as shown in Fig. 1(a). The detailed fabrication process can be found in the experimental section. To obtain high efficiency and reproducibility, it is essential to control the thickness of each layer of the scaffold. To fabricate

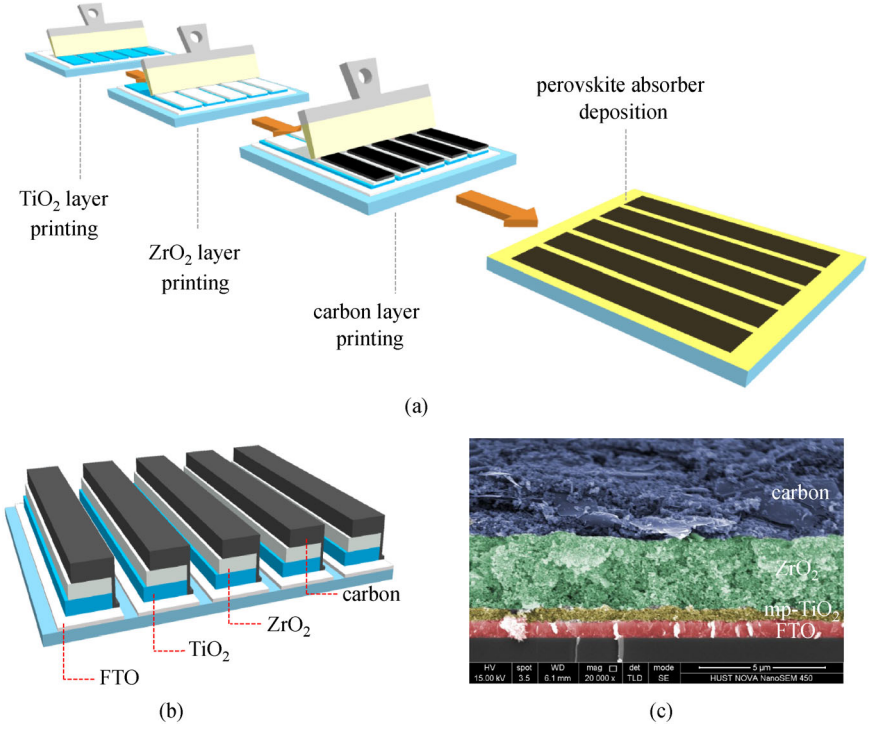

Fig. 1 (a) Scheme of the fabrication process of printable mesoscopic PSCs; (b) structure of the printable mesoscopic PSC submodules with series-connections; (c) cross-sectional SEM image of the screen printed scaffold

large-area submodules, the relative positions of each layer is also important, which need to construct a series-connections for the strip unit cells, as shown in Fig. 1(b). The cross-sectional scanning electron microscopy (SEM) image of the screen printed scaffold is shown in Fig. 1(c).

For printing the TiO_2 layer, the most widely used printing paste is supplied by GreatCell Solar (NR30). However, if the paste is used as received, the thickness of the printed TiO_2 layer is usually 2–3 μm. Of course, the thickness can be tuned by optimizing the mesh and printing parameters, but it is impossible to reduce the thickness to below 1 μm. Thus, we diluted the TiO_2 paste with the solvent of α-terpineol. Since the paste has a very high viscosity, it is more convenient to prepare the samples with mass ratio, not volume ratio. When we diluted the TiO_2 paste with 3.5, 4.0 and 4.5 times of α-terpineol, the thickness of the printed TiO_2 film significantly reduced to 725±16 nm, 636±16 nm and 559±13 nm, as shown in Fig. 2(a). The thickness was measured by a profilometer, and the results were summarized with 9 points on the samples. The statistical distributions of the thickness are shown in Fig. 2(b).

After diluting the TiO_2 paste, the thickness of the screen printed TiO_2 film has successfully reduced to the target value of 500–600 nm. To further study the factors that determine or mainly influence the thickness of the film, we measured the viscosity and solid content of the pastes. At room temperature (RT, 25°C), the TiO_2 paste/terpineol 1:3.5 sample has a viscosity of 286.7 cP. When the ratio of terpineol increased to 4.0 and 4.5, the viscosity of the paste significantly reduced to 237.2 and 196.3 cP. This much reduced viscosity may influence the screen printing process and the film thickness. Particularly, the TiO_2 paste is kept in the refrigerator (4–8°C) for storage. When it was taken out and used, the temperature usually cannot reach RT. Thus, we can observe that the viscosity of the paste varied when we printed it. Whether the viscosity affect the thickness of the printed films remains a critical issue.

We measured the viscosity of the TiO_2 pastes with different terpineol ratio at different temperature, as shown in Fig. 3(b). It was found that the viscosity of the pastes is quite sensitive to the temperature. When the temperature increased from 18°C to 34°C, the viscosity of the pastes reduced from 400–600 cP to 100–150 cP. In the clean room, the temperature is set to 25°C, but there might be a temperature error of at least 2–3°C. In this case, the viscosity of the paste may have a deviation of 10%–20%. To verify whether the viscosity affect the film thickness, we printed TiO_2 films with 1:4.5 paste at different temperatures, as shown in Fig. 3(c). It was found that the film thickness slightly increased 518 to 642 nm when the viscosity of the paste reduced from 397.70 to 80.21 cP. If we can control the temperature variation to be 2–3°C, the variation of the viscosity of the pastes will be < 100 cP. In this case, the variation of the film thickness will be less than 50 nm. In another word, the viscosity of the paste and the printing temperature may influence the film thickness, but are not the main factors. The printed film thickness is determined by the amount of the materials that can go through the screen mesh and transfer to the substrate during the printing process [4]. The lower the viscosity of the paste is, the easier the paste can pass through the screen mesh and transfer to the substrate. Thus, reducing the viscosity of the paste can increase the thickness of the printed films.

More directly, the film thickness is influenced by the solid content of the pastes, as shown in Fig. 3(d). This is the key why the film thickness can dramatically reduce when the pastes were diluted. It is not caused by the reduced viscosity, but the materials than can be transferred to the substrate with the same screen mesh and printing process. The paste may pass through less, but the final solid-state materials on the substrate is much more, leading to increase film thickness.

As mentioned previously, changing the screen mesh with different parameters, such as the mesh count, tension and thread diameter, can also tune the film thickness. Here

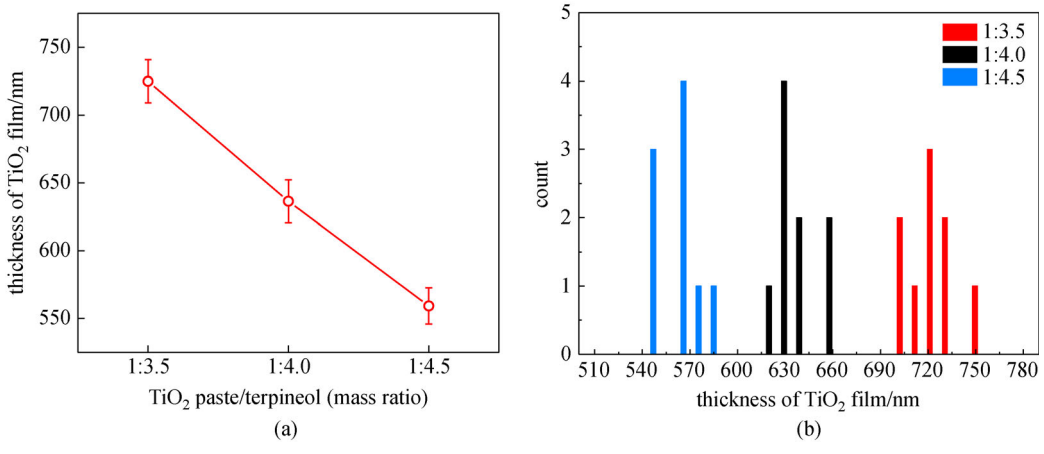

Fig. 2 (a) Thickness variations of the screen printed TiO_2 layer with different paste/terpineol mass ratio; (b) statistical distributions of the thickness

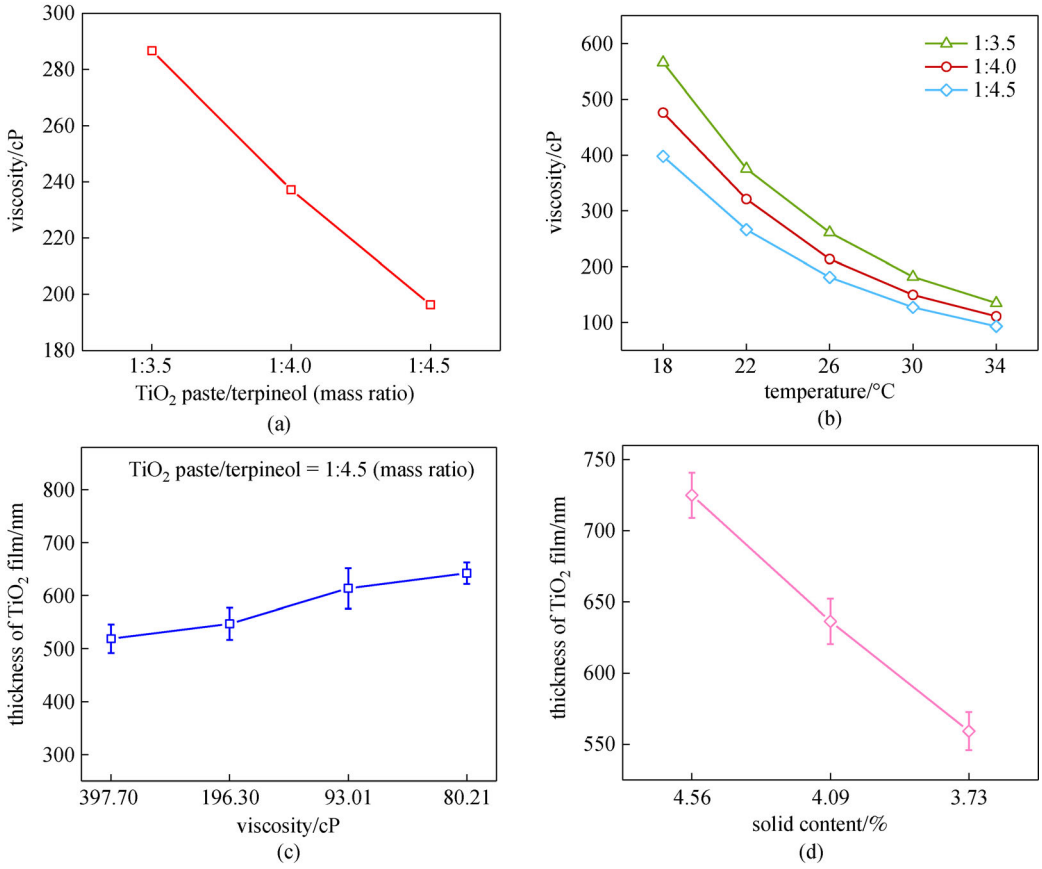

Fig. 3 (a) Dependence of viscosity of the TiO_2 paste on paste/terpineol mass ratio; (b) dependence of viscosity of the TiO_2 paste on temperature; (c) dependence of the TiO_2 layer thickness on the viscosity; (d) dependence of the TiO_2 layer thickness on the solid content

in this work, the mesh count of the screen mesh is 150T mesh/inch. The tension is 25 N/cm, and the diameter of the polyester thread is 45 μm. Besides the screen mesh, the printing parameters also play a key role in controlling the film thickness.

As shown in Fig. 4, the influence of the main printing parameters of print speed, print gap and print pressure on film thickness was investigated. When the print speed decreased from 250 to 50 mm/s, the film thickness reduced from 725±16 to 500±23 nm. As mentioned previously, the film thickness is determined by the amount of the paste that can go through the screen mesh. Here the amount of the paste that can go through the screen mesh is influenced by the deformation of the screen mesh. When the squeegee moves with higher speed, the screen mesh will undergo a more severe deformation, leading to more paste go through the screen mesh and transfer to the substrate. Thus, the higher printing speed will increase the TiO_2 film thickness. The print gap is the distance between the screen mesh and the substrate. When it increased from 2 to 4 mm, the film thickness increased from 649±13 to 757±23 nm. For the print pressure, there is an optimal value for the paste to pass through, obtaining the thickest films. When the pressure is too low, the screen mesh may not be able to contact the substrate tightly, slowing down the transfer of the paste. When the pressure is too high, the screen mesh is squeezed too much, which also suppresses the transfer of the paste from the mesh to the substrate.

Furthermore, we investigated the printing accuracy of the printed TiO_2 films. The screen printer is supplied by SMT-DEK (icon 6), and has a CCD automatic positioning system. For the pastes with different viscosity and solid content, the printing accuracy may vary from 88±8 to 98±9 nm, as shown in Fig. 5(a). We etched the FTO layer on the FTO substrate, forming a target position, as shown in Fig. 5(b). With a microscopy system, it was clear observed that the printed TiO_2 films have quite rough edges. Besides the positional accuracy, we also investigated the printing length accuracy, as shown in Fig. 5(c), which is much smaller than the positional accuracy. This indicates that printing error is not only caused by the spreading of the pastes on the substrate after printing, but also by the printing accuracy of the printer.

Another issue is the edge effect of the printed TiO_2 films, which is widely observed for screen printing technique [36,37]. As shown in Fig. 5(d), the edge of the film (Paste 1, GreatCell Solar, NR30) has an extremely high peak with a thickness of over 1500 nm, while the target thickness of the films is only 500–550 nm. For the sample prepared with paste 2 (purchased from WonderSolar, China), the

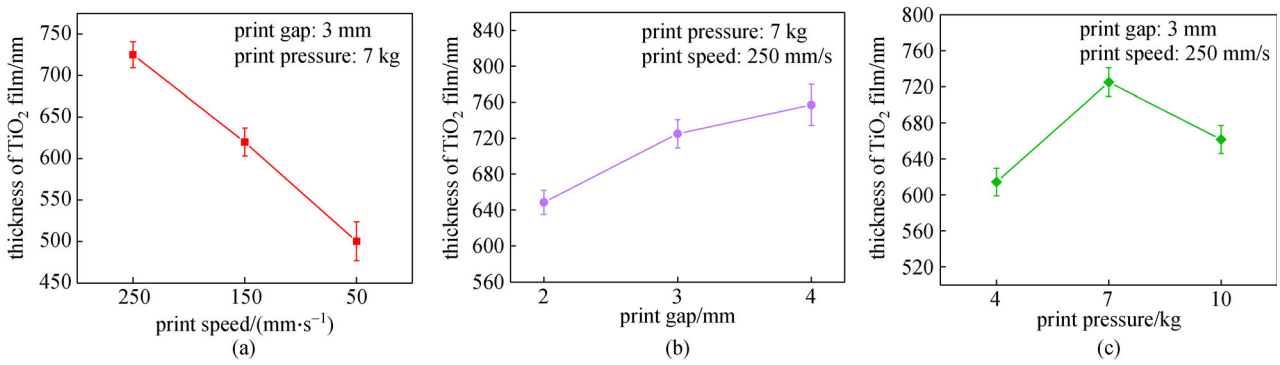

Fig. 4 (a) Dependence of the film thickness on print speed; (b) dependence of the film thickness on print gap; (c) dependence of the film thickness on print pressure

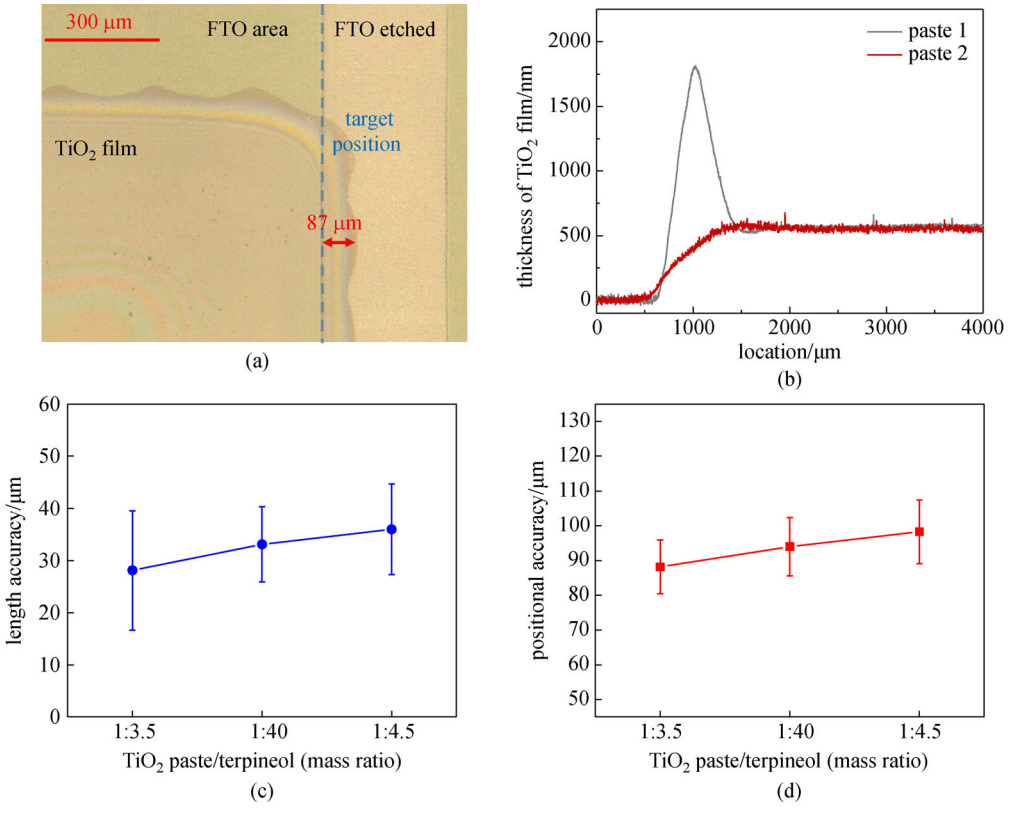

Fig. 5 (a) Positional accuracy for printing the TiO_2 films; (b) microscopy image of the edge of printed TiO_2 films on FTO substrate; (c) length accuracy for printing the TiO_2 films; (d) edge effect of the printed TiO_2 films

edge effect is avoided. Notably, the paste 2 is used as received without long-term storage. The exact causes of the edge-peaks have not been ween identified, but it is highly possible to be related to the aggregation effect of the paste after a long-term storage. Maybe fresh paste 1 can also obtain edge-peak-free TiO_2 films. Now that the edge effect can be effectively avoided, the potential further large-scale production of the such TiO_2 films and printable PSCs be much more practical.

4 Conclusions

We tuned the printing pastes and printing parameters for coating TiO_2 films, and successfully print TiO_2 films with the thickness of 500 – 550 nm. The influence of the solid content and viscosity of the pastes, the temperature, the printing speed, gap and pressure on the film thickness was investigated. It was found that the thickness was determined by the fact that how much paste can be

transferred from the screen mesh to the substrate. The edge effect that the edge of the TiO_2 films possesses a much larger thickness and printing positional accuracy have also been studied. This work will significantly benefit the further development of printable mesoscopic PSCs.

Acknowledgements The authors acknowledge financial support from the National Natural Science Foundation of China (Grant Nos. 21702069, 91433203 and 61474049), the Ministry of Science and Technology of China (863) (No. 2015AA034601), the Fundamental Research Funds for the Central Universities, the Science and Technology Department of Hubei Province (No. 2017AAA190), the 111 Project (No. B07038), the China Postdoctoral Science Foundation (No. 2017M612452), and the Double first-class research funding of China-EU Institute for Clean and Renewable Energy (Nos. ICARE-RP-2018-SOLAR-001 and ICARE-RP-2018-SOLAR-002).

Conflicts of interest
There are no conflicts of interest to declare.

References

1. Rong Y, Ming Y, Ji W, Li D, Mei A, Hu Y, Han H. Toward industrial-scale production of perovskite solar cells: screen printing, slot-die coating, and emerging techniques. Journal of Physical Chemistry Letters, 2018, 9(10): 2707–2713
2. Somalu M R, Muchtar A, Daud W R W, Brandon N P. Screen-printing inks for the fabrication of solid oxide fuel cell films: a review. Renewable & Sustainable Energy Reviews, 2017, 75: 426–439
3. Miller F L. Paste Transfer in the Screening Process. SAE Technical Paper Series, 1968, 680796
4. Towards a better understanding of screen print thickness control: R. J. Horwood. Electrocomponent Science and Technology. 1, 129 (1974). Microelectronics Reliability, 1975, 14(3): 284
5. Späth M, Sommeling P M, van Roosmalen J A M, Smit H J P, van der Burg N P G, Mahieu D R, Bakker N J, Kroon J M. Reproducible manufacturing of dye-sensitized solar cells on a semi-automated baseline. Progress in Photovoltaics: Research and Applications, 2003, 11(3): 207–220
6. Wenham S R, Green M A. Silicon solar cells. Progress in Photovoltaics: Research and Applications, 1996, 4(1): 3–33
7. Ito S, Murakami T N, Comte P, Liska P, Grätzel C, Nazeeruddin M K, Grätzel M. Fabrication of thin film dye sensitized solar cells with solar to electric power conversion efficiency over 10%. Thin Solid Films, 2008, 516(14): 4613–4619
8. O'Regan B, Grätzel M. A low-cost, high-efficiency solar cell based on dye-sensitized colloidal TiO2 films. Nature, 1991, 353: 737–740
9. Hagfeldt A, Boschloo G, Sun L, Kloo L, Pettersson H. Dye-sensitized solar cells. Chemical Reviews, 2010, 110(11): 6595–6663
10. Hinsch A, Brandt H, Veurman W, Hemming S, Nittel M, Würfel U, Putyra P, Lang-Koetz C, Stabe M, Beucker S. Dye solar modules for facade applications: recent results from project ColorSol. Solar Energy Materials and Solar Cells, 2009, 93(6–7): 820–824
11. Hinsch A, Veurman W, Brandt H, Loayza Aguirre R, Bialecka K, Flarup Jensen K. Worldwide first fully up-scaled fabrication of 60 × 100 cm^2 dye solar module prototypes. Progress in Photovoltaics: Research and Applications, 2012, 20(6): 698–710
12. Pettersson H, Gruszecki T, Schnetz C, Streit M, Xu Y, Sun L, Gorlov M, Kloo L, Boschloo G, Häggman L, Hagfeldt A. Parallel-connected monolithic dye-sensitised solar modules. Progress in Photovoltaics: Research and Applications, 2010, 18(5): 340–345
13. Rong Y, Liu G, Wang H, Li X, Han H. Monolithic all-solid-state dye-sensitized solar cells. Frontiers of Optoelectronics, 2013, 6(4): 359–372
14. Kato N, Takeda Y, Higuchi K, Takeichi A, Sudo E, Tanaka H, Motohiro T, Sano T, Toyoda T. Degradation analysis of dye-sensitized solar cell module after long-term stability test under outdoor working condition. Solar Energy Materials and Solar Cells, 2009, 93(6–7): 893–897
15. Dai S, Weng J, Sui Y, Chen S, Xiao S, Huang Y, Kong F, Pan X, Hu L, Zhang C, Wang K. The design and outdoor application of dye-sensitized solar cells. Inorganica Chimica Acta, 2008, 361(3): 786–791
16. Takeda Y, Kato N, Higuchi K, Takeichi A, Motohiro T, Fukumoto S, Sano T, Toyoda T. Monolithically series-interconnected transparent modules of dye-sensitized solar cells. Solar Energy Materials and Solar Cells, 2009, 93(6–7): 808–811
17. Kojima A, Teshima K, Shirai Y, Miyasaka T. Organometal halide perovskites as visible-light sensitizers for photovoltaic cells. Journal of the American Chemical Society, 2009, 131(17): 6050–6051
18. Kim H S, Lee C R, Im J H, Lee K B, Moehl T, Marchioro A, Moon S J, Humphry-Baker R, Yum J H, Moser J E, Grätzel M, Park N G. Lead iodide perovskite sensitized all-solid-state submicron thin film mesoscopic solar cell with efficiency exceeding 9%. Scientific Reports, 2012, 2(1): 591
19. Yang W S, Park B W, Jung E H, Jeon N J, Kim Y C, Lee D U, Shin S S, Seo J, Kim E K, Noh J H, Seok S I. Iodide management in formamidinium-lead-halide-based perovskite layers for efficient solar cells. Science, 2017, 356(6345): 1376–1379
20. Bi D, Yi C, Luo J, Décoppet J D, Zhang F, Zakeeruddin S M, Li X, Hagfeldt A, Grätzel M. Polymer-templated nucleation and crystal growth of perovskite films for solar cells with efficiency greater than 21%. Nature Energy, 2016, 1(10): 16142
21. Rong Y, Hu Y, Mei A, Tan H, Saidaminov M I, Seok S I, McGehee M D, Sargent E H, Han H. Challenges for commercializing perovskite solar cells. Science, 2018, 361(6408): eaata8235
22. Green M A, Hishikawa Y, Dunlop E D, Levi D H, Hohl-Ebinger J, Yoshita M, Ho-Baillie A W Y. Solar cell efficiency tables (Version 53). Progress in Photovoltaics: Research and Applications, 2019, 27 (1): 3–12
23. Rong Y, Liu L, Mei A, Li X, Han H. Beyond efficiency: the challenge of stability in mesoscopic perovskite solar cells. Advanced Energy Materials, 2015, 5(20): 1501066
24. Hu Y, Si S, Mei A, Rong Y, Liu H, Li X, Han H. Stable large-area (10 × 10 cm^2) printable mesoscopic perovskite module exceeding 10% efficiency. Solar RRL, 2017, 1(2): 1600019
25. Rong Y, Hou X, Hu Y, Mei A, Liu L, Wang P, Han H. Synergy of ammonium chloride and moisture on perovskite crystallization for efficient printable mesoscopic solar cells. Nature Communications, 2017, 8: 14555
26. Yin G, Ma J, Jiang H, Li J, Yang D, Gao F, Zeng J, Liu Z, Liu S F. Enhancing efficiency and stability of perovskite solar cells through

Nb-doping of TiO_2 at low temperature. ACS Applied Materials & Interfaces, 2017, 9(16): 14545
27. Jiang Y, Leyden M R, Qiu L, Wang S, Ono L K, Wu Z, Juarez-Perez E J, Qi Y. Combination of hybrid CVD and cation exchange for upscaling Cs-substituted mixed cation perovskite solar cells with high efficiency and stability. Advanced Functional Materials, 2018, 28(1): 1703835
28. Liu T, Chen K, Hu Q, Zhu R, Gong Q. Inverted perovskite solar cells: progresses and perspectives. Advanced Energy Materials, 2016, 6(17): 1600457
29. Luo D, Yang W, Wang Z, Sadhanala A, Hu Q, Su R, Shivanna R, Trindade G F, Watts J F, Xu Z, Liu T, Chen K, Ye F, Wu P, Zhao L, Wu J, Tu Y, Zhang Y, Yang X, Zhang W, Friend R H, Gong Q, Snaith H J, Zhu R. Enhanced photovoltage for inverted planar heterojunction perovskite solar cells. Science, 2018, 360(6396): 1442–1446
30. Ku Z, Rong Y, Xu M, Liu T, Han H. Full printable processed mesoscopic $CH_3NH_3PbI_3/TiO_2$ heterojunction solar cells with carbon counter electrode. Scientific Reports, 2013, 3(1): 3132
31. De Rossi F, Baker J A, Beynon D, Hooper K E A, Meroni S M P, Williams D, Wei Z, Yasin A, Charbonneau C, Jewell E H, Watson T M. All printable perovskite solar modules with 198 cm^2 active area and over 6% efficiency. Advanced Materials Technologies, 2018, 3 (11): 1800156
32. Baranwal A K, Kanaya S, Peiris T A N, Mizuta G, Nishina T, Kanda H, Miyasaka T, Segawa H, Ito S. 100°C thermal stability of printable perovskite solar cells using porous carbon counter electrodes. ChemSusChem, 2016, 9(18): 2604–2608
33. Grancini G, Roldán-Carmona C, Zimmermann I, Mosconi E, Lee X, Martineau D, Narbey S, Oswald F, De Angelis F, Graetzel M, Nazeeruddin M K. One-year stable perovskite solar cells by 2D/3D interface engineering. Nature Communications, 2017, 8: 15684
34. Chan C Y, Wang Y, Wu G W, Wei-Guang Diau E. Solvent-extraction crystal growth for highly efficient carbon-based mesoscopic perovskite solar cells free of hole conductors. Journal of Materials Chemistry A, Materials for Energy and Sustainability, 2016, 4(10): 3872–3878
35. Liu T, Liu L, Hu M, Yang Y, Zhang L, Mei A, Han H. Critical parameters in TiO_2/ZrO_2/Carbon-based mesoscopic perovskite solar cell. Journal of Power Sources, 2015, 293: 533–538
36. Deegan R D, Bakajin O, Dupont T F, Huber G, Nagel S R, Witten T A. Capillary flow as the cause of ring stains from dried liquid drops. Nature, 1997, 389(6653): 827–829
37. Lin H W, Chang C P, Hwu W H, Ger M D. The rheological behaviors of screen-printing pastes. Journal of Materials Processing Technology, 2008, 197(1–3): 284–291

Zhining Wan is a master student at Wuhan National Laboratory for Optoelectronics (WNLO)/Huazhong University of Science and Technology (HUST). He received his B.S. degree from Wuhan University of Science and Technology in 2016. His main research is focused on screen printing techniques for printable mesoscopic perovskite solar cells.

Mi Xu is a postdoctoral researcher at Wuhan National Laboratory for Optoelectronics (WNLO)/Huazhong University of Science and Technology (HUST). He received his B.S. degree in Material Physics from Wuhan University in 2009, and Ph.D. degree in Optics Engineering from HUST in 2014. He then worked in a commercial company and studied on OLED with solution process. In 2016, he joined WNLO/HUST. His main research interests include perovskite solar cells, mesoscopic structure materials, and solution process technology.

Da Li is a master student at Wuhan National Laboratory for Optoelectronics (WNLO)/Huazhong University of Science and Technology (HUST). He received his B.S. degree in Materials Science and Engineering from China University of Geosciences in 2017. His main research interests include the fabrication and interface modification of perovskite solar cells.

Zhengyang Fu is a master student at Wuhan National Laboratory for Optoelectronics (WNLO)/Huazhong University of Science and Technology (HUST). He received his B.S. degree from Yunnan University in 2015, His main research interests include the encapsulation and stability of mesoscopic perovskite solar cells.

Anyi Mei is an associate professor at Wuhan National Laboratory for Optoelectronics (WNLO)/Huazhong University of Science and Technology (HUST). He received his B.E. degree in Materials Science and Engineering (2013) and Ph. D. degree in Optical Engineering (2018) from HUST. His research interests are focused on printable mesoscopic perovskite solar cells and related materials.

Yue Hu is an associate professor at Wuhan National Laboratory for Optoelectronics (WNLO)/Huazhong University of Science and Technology (HUST). She received her B.S. degree in Applied Chemistry from East China University of Science and Technology (ECUST) in 2012, and Ph.D. degree in Chemistry from University of Edinburgh in 2016. Her current research focuses on designing and synthesizing novel organic-inorganic hybrid perovskite materials and photovoltaics.

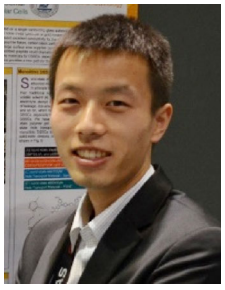

Yaoguang Rong is an associate professor at Wuhan National Laboratory for Optoelectronics (WNLO)/Huazhong University of Science and Technology (HUST). He received his B.S. degree in Material Physics from Wuhan University in 2009, and Ph.D. degree in Optics Engineering from HUST in 2014. He then worked as a postdoctoral researcher at University of Houston (the United States). In 2016, he joined WNLO/HUST. His main research interests include perovskite solar cells, dye-sensitized solar cells, and mesoscopic structure materials.

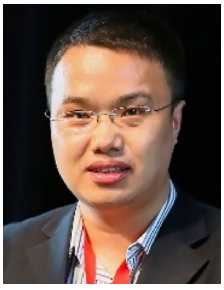

Hongwei Han is Professor at Wuhan National Laboratory for Optoelectronics (WNLO), Huazhong University of Science and Technology (HUST) in China. He received his B.S. degree in Applied Chemistry and his Ph.D. degree in Condensed Matter Physics from Wuhan University in 2000 and 2005, respectively. Later, he stayed in Wuhan University as lecturer. And then he worked as postdoctoral research fellow at Monash University in Australia for two years. After that he joined HUST and WNLO in 2008 and began to establish his group of Printable Mesoscopic Photovoltaics & Optoelectronics. Since 2000, Dr. Han has worked on the fully printable mesoscopic solar cells. His more than 80 peer-reviewed publications in *Science*, *Nature Chemistry*, *Nature Communications*, *J. Am. Chem. Soc.* etc. have been published and 22 Patents have been applied within past five years. His research interests are printable photovoltaics and optoelectronics, especially printable mesoscopic solar cells.